Title

Nanoparticle delivery of siRNA against TWIST to reduce drug resistance and tumor growth in ovarian cancer models

Journal

Nanomedicine Nanotechnology Biology and Medicine, 13(3)

ISSN

1549-9634

Authors

Roberts, Cai M
Shahin, Sophia Allaf
Wen, Wei
et al.

Publication Date

2017-04-01

DOI

10.1016/j.nano.2016.11.010

Peer reviewed

HHS Public Access

Author manuscript

Nanomedicine. Author manuscript; available in PMC 2022 April 12.

Published in final edited form as:

Nanomedicine. 2017 April ; 13(3): 965–976. doi:10.1016/j.nano.2016.11.010.

Nanoparticle delivery of siRNA against TWIST to reduce drug resistance and tumor growth in ovarian cancer models

Cai M. Roberts[a,b,*], **Sophia Allaf Shahin**[a,b,*], **Wei Wen**[c], **James B. Finlay**[a,b,1], **Juyao Dong**[c,2], **Ruining Wang**[c], **Thanh H. Dellinger**[d], **Jeffrey I. Zink**[c], **Fuyuhiko Tamanoi**[e], **Carlotta A. Glackin**[b,**]

[a]Irell & Manella Graduate School of Biological Sciences, City of Hope – Beckman Research Institute, 1500 E. Duarte Road, Duarte, California 91010, USA

[b]Department of Stem Cell and Developmental Biology, City of Hope – Beckman Research Institute, 1500 E. Duarte Road, Duarte, California 91010, USA

[c]Department of Chemistry and Biochemistry, Jonsson Comprehensive Cancer Center, California NanoSystems Institute, University of California Los Angeles, 405 Hilgard Avenue, Los Angeles, California 90095–1569, USA

[d]Department of Surgery, City of Hope – Beckman Research Institute, 1500 E. Duarte Road, Duarte, California 91010, USA

[e]Department of Microbiology, Immunology, and Molecular Genetics, Jonsson Comprehensive Cancer Center, California NanoSystems Institute, University of California Los Angeles, 405 Hilgard Avenue, Los Angeles, California 90095–1569, USA

Abstract

Epithelial ovarian cancer (EOC) is the most deadly gynecologic malignancy on account of its late stage at diagnosis and frequency of drug resistant recurrences. Novel therapies to overcome these barriers are urgently needed. TWIST is a developmental transcription factor reactivated in cancers and linked to angiogenesis, metastasis, cancer stem cell phenotype, and drug resistance, making it a promising therapeutic target. In this work, we demonstrate the efficacy of TWIST siRNA (siTWIST) and two nanoparticle delivery platforms to reverse chemoresistance in EOC models. Polyamidoamine dendrimers and mesoporous silica nanoparticles (MSNs) carried siTWIST into target cells and led to sustained TWIST knockdown *in vitro*. Mice treated with cisplatin plus MSN-siTWIST exhibited lower tumor burden than mice treated with cisplatin alone, with most of the effect coming from reduction in disseminated tumors. This platform has potential application

[**]Corresponding author Carlotta A. Glackin, cglackin@coh.org, Tel: (+1)626-256-4673.

[1]Present address: Department of Animal Resources, University of Southern California, 1540 Alcazar St., CHP 234, Los Angeles, CA 90033

[2]Present address: Department of Chemical Engineering, Massachusetts Institute of Technology, 77 Massachusetts Avenue, Cambridge, Massachusetts 02139

[*]These authors contributed equally to this work

for overcoming the clinical challenges of metastasis and chemoresistance in EOC and other TWIST overexpressing cancers.

Graphical Abstract

siRNA targeting TWIST can be complexed by electrostatic interactions with either a third generation polyamidoamine (PAMAM) dendrimer micelle or polyethyleneimine (PEI) coated mesopourous silica nanoparticle (MSN). Delivery of the siRNA payload into Ovcar8 cells resulted in substantial TWIST knockdown and sensitization of cells to cisplatin treatment. *In vivo* studies demonstrated that MSNs carrying TWIST siRNA combined with cisplatin produced greater reduction in tumor burden than cisplatin alone.

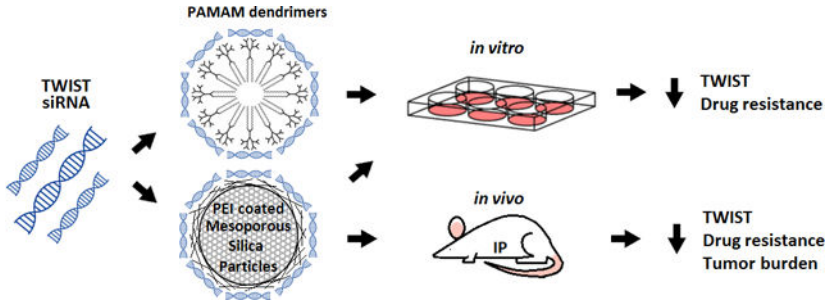

Keywords

TWIST; siRNA; mesoporous silica nanoparticles; polyamidoamine dendrimers; ovarian cancer

Background

Epithelial ovarian cancer (EOC) is one of the leading causes of cancer-related deaths among women worldwide, representing a significant unmet therapeutic challenge [1–3]. EOC accounts for 90% of all ovarian cancers [1]; additionally, 70% of women with EOC are not diagnosed until the disease is advanced stage [1]. The majority of EOC patients respond well to first line chemotherapy consisting of a platinum drug and/or paclitaxel. Unfortunately, most of these patients relapse with disease that is both metastatic and drug resistant, with a five-year survival rate of approximately 20% [3–5]. There is therefore an urgent need for therapies to prevent both metastatic spread and acquired drug resistance in EOC.

EOC tumors are characterized by high expression levels of epithelial-to-mesenchymal transition (EMT) markers such as *TWIST*, which plays an essential role in cancer metastasis (Figure 1A) [6,7]. Overexpression of *TWIST* or changes to its promoter methylation state are common in metastatic carcinomas, including EOC [7–9]. In addition, TWIST and EMT are responsible for regulating chemoresistance and cancer cell stemness [10–12]. TWIST upregulates EMT effectors such as N-cadherin and vimentin, and downregulates E-cadherin (Figure1B) [13]. It has been previously shown that knockdown of *TWIST* target genes results in decreased tumor burden and angiogenesis in a melanoma model [14], and reduces the invasive phenotype in triple-negative breast cancer [15]. However, transcription factors such as TWIST are difficult to target with small molecule drugs due to their nuclear

localization [16]. To circumvent this issue, small interfering RNAs (siRNAs) have become increasingly popular. We have designed and validated two therapeutic siRNAs against *TWIST* (Figure 1C), and have evaluated two nanoparticle-based delivery platforms. First, we used third generation polyamidoamine (PAMAM) dendrimers, and second, we created polyethylenimine (PEI) coated mesoporous silica nanoparticles (MSNs). We have previously shown effective delivery to tumor cells using both of these modalities, both *in vitro* and in mouse models of melanoma and breast cancer [14,15].

In this study we applied our siRNA-nanoparticle technologies to EOC. We hypothesized that nanoparticle delivered anti-TWIST siRNAs would knock down *TWIST* and sensitize cells to chemotherapeutics. We also evaluated the tumor-specific delivery capability of our MSNs. By evaluating the effects of TWIST knockdown using MSNs in animal models of a metastatic and chemoresistant phenotype, we present an MSN delivery platform for siRNA and drug combination therapies to prevent both metastatic spread and acquired drug resistance in ovarian and other cancers.

Methods

Cell Culture

A2780R and all derivatives of Ovcar8 were grown in RPMI 1640 (Genesee Scientific, San Diego, CA) in a tissue culture incubator at 37°C, 5% CO_2, and 90% humidity. Growth medium was supplemented with 10% fetal bovine serum and 1% penicillin/streptomycin. Cells were passaged every 2–4 days using 0.25% trypsin (Genesee Scientific). Where indicated, cells were transfected with Lipofectamine 2000 (Thermo Fisher, Waltham, MA) according to the manufacturer's instructions. A2780R cells are a cisplatin resistant derivative of A2780 and were a gift from Dr. John Yim's lab at City of Hope.

Optimization of Ovcar8 for in vivo *use*

For mouse experiments, Ovcar8 cells were stably transfected with CMV-p:EGFP-ffluc pHIV7 (a gift from Christine Brown at City of Hope) as has been described previously [17]. This resulted in expression of an eGFP-firefly luciferase (ffluc) fusion protein. To increase engraftment efficiency and homogeneity of the cell population, Ovcar8 cells were passaged through mice. Ovcar8-GFP+ffluc cells were injected intraperitoneally (IP) and allowed to form tumors. Cells were harvested after 37 days and used to establish the Ovcar8-IP line.

siRNA design

siRNAs against TWIST were designed based on shRNAs that were previously validated [13,15]. Sequences are: si419 guide, 5'-AAUCUUGCUCAGCUUGUCCUU-3'; si419 passenger, 5'-GGACAAGCUGAGCAAGAUU-3'; si494 guide, 5'-UUGGAGUCCAGCUCGUCGCUU-3'; si494 passenger, 5'-GCGACGAGCUGGACUCCAA-3'. Non-targeting control siRNA (siQ) was AllStars Negative Control siRNA, labeled with AlexaFluor-647, from Qiagen (Valencia, CA). For *in vivo* studies, 2'-O-methyluracil and inverted abasic ribose chemical modifications were made to the si419 passenger strand, as illustrated in Figure 4A [14].

PAMAM dendrimer design and delivery

The polyamidoamine (PAMAM) dendrimer used in this study is the YTZ3–5 third generation dendrimer, illustrated in Figure 2A and previously described [15,18]. To complex the dendrimer with siRNA, YTZ3–15 at 240 μM was mixed with 10 μM siRNA in OptiMEM Low Serum Medium (Thermo Fisher). Upon complexing with siRNA, dendrimers form micelle structures with siRNA at the surface and the hydrophobic tails sequestered in the core (Figure 2B) [19]. 14.6 μl YTZ3–15 and 10 μl siRNA were used per well of a 6-well plate. Final concentrations of YTZ3–15 and siRNA once added to cells were 1.75 μM and 50 nm, respectively. Where indicated, 3.5 μM YTZ3–15 and 100 nm siRNA were used for Ovcar8.

MSN design and delivery

Mesoporous silica nanoparticles (MSNs) were synthesized utilizing the sol-gel method as described previously [14,20]. First, 250 mg 95% cetyltrimethylammonium bromide (CTAB) was dissolved in 120 ml of water with 875 μl 2M sodium hydroxide solution, at 80°C. Next, 1.2 ml of 98% tetraethylorthosilicate was added. After 15 min, 300 μl of 42% 3-(trihydroxysilyl) propyl methylphosphonate was added, and the mixture was stirred 2 hr. Particles were collected using centrifugation and washed with methanol. Acidic methanol was then used to remove any remaining CTAB surfactants. Zeta potential at 50 μg/mL was 43.75 mV [14]. All chemicals were obtained from Aldrich (St. Louis, MO). Particles were ~120 nm in diameter, with 2.5 nm pores. Low molecular weight (1.8 kD branched polymer) polyethyleneimine (PEI) was electrostatically attached to the particle surface to provide a positive change to attract negatively charged siRNA [21]. To complex siRNA for *in vitro* experiments, 10 μl siRNA at 10 μM was mixed with 70 ul MSNs at 500 μg/ml and 20 μl water, and the mixture was incubated overnight at 4°C on a roller. The following day, 100 μl of the MSN-siRNA complexes was added to each well of a 6-well plate containing 1900 μl normal medium.

Fluorescence Microscopy

To verify cell uptake of the nanoparticle-siRNA complexes, cells were imaged immediately before harvesting. Phase images were acquired, as well as fluorescent images to detect siQ-AlexaFluor-647. Images were acquired using a Nikon TE-2000S microscope and SPOT Advanced software (Diagnostic Instruments, Sterling Heights, MI).

Confocal Microscopy

Ovcar8-IP cells were seeded into a 3.5 cm glass bottom tissue culture dish. Following attachment (24 hr), 2 ml of fresh medium replaced the old medium. Next, MSN + siQ complexes (labeled with AlexaFluor® 647) were added to the cells in the dish at final concentrations of 17.5 ng/μl (MSN) and 50 nM (siQ) and incubated for an additional 48 hours in a tissue culture incubator. Cells were then treated with LysoTracker Red (Thermo Fisher Scientific, Waltham, MA) according to the manufacturer's protocol. Confocal images were obtained using the Zeiss LSM700 Confocal Microscope and ZEN 2012 microscopy software (Zeiss AG, Oberkochen, Germany).

Western Blotting

Following siRNA treatment, cells were pelleted and lysed in RIPA buffer. Protein concentration was determined by BCA assay (Thermo Fisher). Following SDS-PAGE, protein was transferred to Amersham PVDF membrane (Genesee Scientific) using a BioRad Trans-Blot SD semi-dry transfer unit. Blots were then blocked in milk for one hour at room temperature or overnight at 4°C. Incubation with primary antibody took place for one hour at room temperature or overnight at 4°C. Antibodies were diluted in 5% milk, with 0.1–0.2% Tween-20. Antibodies used were TWIST 2c1a (Santa Cruz Biotechnology, Dallas, TX) at 1:250–1:500 dilution, β-Actin, A1978 (Sigma Aldrich, St. Louis, MO) at 1:2500–1:5000 dilution; and Horseradish Peroxidase (HRP) conjugated anti-mouse secondary antibodies. For film-based westerns, Blue Devil film (Genesee Scientific) and ECL Plus chemiluminescent substrate (Thermo Fisher) were used to detect protein. For digital westerns, the Syngene Pxi4 digital blot imager and Michigan Diagnostics FemtoGlow chemilumescent substrate were used.

Sulphorhodamine B Cell Survival Assays

A2780R or Ovcar8-IP cells were plated in 6 well plates and allowed to adhere overnight. The following day, cells were transfected with siQ, si419, or si494 as described above - A2780R cells using YTZ3–15 and Ovcar8-IP cells using MSNs. After 48–72 hours, cells were transferred to 96 well plates at 5,000 cells per well and allowed to adhere overnight. The following day cells were treated with cisplatin at a series of concentrations (cells not treated with cisplatin served as controls). After 72 hours, cells were fixed in 10% trichloroacetic acid for 1 hour at 4°C, washed with water, and dried. Cells were stained in 0.4% sulphorhodamine B (SRB) in 1% acetic acid for 15 minutes at room temperature and then washed 3–4 times with 1% acetic acid until no further color was present in the wash. Any stray SRB on the walls of the wells was removed, and stained cells were dried for 10 minutes. SRB was solubilized in 10 mM Tris base and color intensity was quantified by absorbance at 570 nm. Each condition was normalized to its own untreated control.

Animal Studies

The animal studies conducted in these experiments were done in accordance with a protocol approved by the Institutional Animal Care and Use Committee at the City of Hope Beckman Research Institute. A total of 48 female NOD.Cg-*Prkdc*^{scid}*Il2rg*^{tm1Wjl}/SzJ (NSG) mice (The Jackson Laboratory, Bar Harbor, ME) were used. Ten week old (on average) mice were administered an intraperitoneal injection (IP) of 2.5×10^6 Ovcar8-IP cells in 200 μl of RPMI media. For all studies, mice were placed into four groups: MSN-siQ, MSN-siQ + cisplatin, MSN-si419H, and MSN-si419H + cisplatin (n=4 or n=8). Previous reports show no cellular uptake without MSNs [14], thus a siRNA-only group was not added to this study.

Bioluminescent imaging of mice (using Xenogen IVIS 100 biophotonic imaging system, STTARR, Toronto, Ontario, Canada) commenced seven days after injection of tumor cells in order to ensure engraftment, and continued once a week for four weeks. Mice were given a 100 μl IP injection of 20 mg/ml D-Luciferin (PerkinElmer, Waltham, MA). Ten minutes after the D-luciferin injection, mice were anesthetized with isoflurane (2%−5%) and placed in the biophotonic imager, and images were taken within two minutes. An alfalfa-free

version of the regular rodent diet (alfalfa-free CA-1) was administered to the siQ mice to prevent autofluorescence from the regular diet.

IP injections of MSN + siRNA (siQ fluorescently labeled with AlexaFluor® 647 or si419H) were conducted one week after the inoculation of Ovcar8-IP cells and done once or twice per week for a total of four weeks. Mice received 105 μl of 500 ng/μl MSN complexed with 15 μl of 10 μM siRNA per week, divided into one full or two half doses (n=4 and n=8, respectively). This is equivalent to 0.04 mg/kg MSN/week. Weekly 3mg/kg IP cisplatin injections were given starting two weeks after initial inoculation of cells.

At completion of the experiment, all animals were euthanized via CO_2 asphyxiation. Both primary tumors and disseminated masses were carefully dissected from adjacent tissue and weighed. Mice treated twice weekly with siQ only were imaged for biodistribution studies. Tumors, spleen, kidney, uterus and liver were imaged *ex vivo* to detect the location of both the Ovcar8-IP cells and AlexaFluor 647-labeled siQ without the hindrance of the skin and fur. Efficacy data is presented from mice dosed once per week with MSN-siRNA.

Statistics

All *in vivo* data was analyzed using one-way ANOVA with correction for multiple comparisons, comparing all groups to MSN-siQ treatment group. Additionally, an unpaired t-test with Welch's correction was used to compare tumor number and weight between cisplatin alone and the combination cisplatin + MSN-si419H treatment groups. All analyses were done using Prism 6 software (GraphPad Software, La Jolla, CA). * $p < .05$, ** $p < .01$, *** $p < .001$, **** $p < .0001$ throughout. Power analysis demonstrates that 4 mice per group has 99% power to detect a 50% difference in means, assuming 25% standard deviation and a one-tailed test (alpha = 0.05).

Results

Dendrimer delivered siRNA knocks down TWIST in ovarian cancer cell lines

We have previously showed the efficacy of our siRNAs targeting TWIST (si419 and si494, Figure 1C) [14,15]. We used Lipofectamine 2000 transfection to test si419 and si494 in A2780R cells. Both were able to completely inhibit TWIST expression over the course of three days (Figure 1D). In the absence of a carrier, no siRNA enters cells (Figure 1E), therefore once siRNAs had been validated, we introduced the amphiphilic PAMAM dendrimer YTZ3–15 as a delivery vehicle. YTZ3–15 electrostatically attracts negatively charged siRNA using the cationic terminal amines (Figure 2A), while the lipid tails mediate arrangement into micelles (Figure 2B) [19]. In order to verify that dendrimers successfully delivered siRNA into target cells, we conjugated YTZ3–15 with AlexaFluor-647 tagged siQ control siRNA. Micrographs revealed robust cell uptake of labeled siRNA in both A2780R and Ovcar8 cells (Figure 2C). Furthermore, YTZ3–15 delivery of si419 and si494 successfully knocked down TWIST in both lines, although knockdown in Ovcar8 was minimal and required double the usual siRNA-YTZ3–15 dose (Figure 2D).

TWIST knockdown impacts cisplatin resistance

In order to determine the effect of TWIST knockdown on cisplatin resistance, we performed a sulphorhodamine B (SRB) cell survival assay. Following treatment with YTZ3–15-si494, cisplatin resistant A2780R cells were sensitized to cisplatin, with approximately one log difference in IC_{50} (Figure 2E).

Mesoporous Silica Nanoparticles as siRNA delivery vehicles

While YTZ3–15 treatment yielded significant TWIST knockdown in A2780R, we wanted to explore additional nanocarriers which would be capable of multiple functions (i.e. drug delivery and targeting via surface moieties) and have increased efficacy in Ovcar8. Following our recent success using mesoporous silica nanoparticles (MSNs) to target TWIST *in vitro* and *in vivo* in melanoma [14], we elected to apply these particles to EOC. MSNs coated with polyethyleneimine (PEI) can carry siRNA on their outer surface, and contain a pore structure capable of carrying additional cargo, such as cytotoxic drugs (Figure 3A) [20–22]. In addition, MSNs can be modified with controlled release valves and targeting moieties, further increasing their appeal [23–28]. For the present study, we used PEI coated MSNs without additional modifications or drug loading. These particles were of ~120 nm diameter with highly uniform size (Figure 3B). We first confirmed that PEI-coated MSNs could effectively deliver AlexaFluor-647 labeled siQ to both A2780R and Ovcar8 cells (Figure 3C). We found that MSNs required extended incubation with cells to produce knockdown as compared to YTZ3–15, but MSN knockdown lasted longer. With MSNs, we observed little effect at 24 hours but robust knockdown of TWIST lasting up to one week post transfection in both cell lines tested (Figure 3D).

Optimization of siRNAs for in vivo *use by chemical modifications*

In order to maximize siRNA efficacy *in vivo*, nuclease degradation of siRNA and immune activation by siRNAs must be reduced. Immune reactions are mediated largely by toll-like receptors, which respond to varying degrees to different RNA sequence motifs [29]. Analysis of these motifs revealed that si419's passenger strand, which would not be incorporated into RISC, contained no immune-activating sequences, and this siRNA was therefore selected for *in vivo* experiments. We added additional chemical modifications to the si419 passenger strand to create si419 hybrid siRNA (si419H, Figure 4A). In order to promote nuclease resistance of the siRNA duplex, 2'-O-methyl and inverted abasic ribose (iaB) modifications were added [30,31]. iaB also prevents the loading of the passenger strand into RISC, effectively increasing the potency of siRNA by ensuring that all duplexes result in binding to TWIST mRNA, improving silencing [30].

MSNs deliver siRNA to correct cellular compartment of Ovcar8-IP cells

Ovcar8 cells were selected for further study as their genetic makeup more closely resembles that of the typical clinical high grade serous ovarian carcinoma, than the A2780 cell line family [32]. In order to improve uniform tumor cell engraftment in mice and enable tracking of cells *in vivo*, we passaged Ovcar8 cells through mice and used lentiviral transduction to stably express an eGFP firefly luciferase fusion protein (see Methods). This line is hereafter referred to as Ovcar8-IP. Confocal microscopy revealed that MSN treatment of Ovcar8-IP

cells resulted in siQ accumulating in the late endosomes and lysosomes of the cells, as evidenced by colocalization with LysoTracker dye (Figure 4B). These structures are located in the perinuclear space, as we have shown previously [14,15]. Transfection of Ovcar8-IP cells using MSNs and si419H resulted in robust knockdown of TWIST even after 24 hours of treatment (Figure 4C). Furthermore, SRB assays revealed sensitization of Ovcar8-IP cells to cisplatin following MSN-419H or MSN-419 treatment (Figure 4D). Ovcar8 cells are not as cisplatin resistant as A2780R, hence a smaller effect size compared to that seen in Figure 2E.

MSNs selectively accumulate in disseminated Ovcar8-IP masses

In order to determine if our MSNs targeted tumors *in vivo,* we performed fluorescent imaging of siQ treated mice. Ovcar8-IP cells successfully produced primary tumors (defined as those localized to the ovary) and disseminated masses (Figure 5, C and D). This pattern of engraftment following IP administration of cells is consistent with the current prevailing theory that the site of origin for EOC is the fallopian tube epithelium, and that cells migrate to the ovary and peritoneal cavity, giving rise to both large ovarian tumors and widely disseminated tumor foci [33–35]. MSNs carrying siRNA selectively penetrated and accumulated at these primary tumors and disseminated masses, but not in any other peritoneal tissue or organ examined (Figure 5, E and F). Note that a tumor focus also appears on the liver of this control mouse, to which the MSN-siQ also homed (Figure 5, D and F). Tumor uptake of MSN-siQ was greater in disseminated masses than in ovaries, but signal is visible on the primary tumors.

Ovcar8-IP tumor growth is inhibited by siTWIST and cisplatin combination therapy

Mice were treated weekly for four weeks with MSN-siQ or MSN-si419H, with or without cisplatin. After four weeks of therapy, the negative control (MSN-siQ weekly) mice developed significant tumors and produced disseminated masses as shown by relative bioluminescent photon flux measurements (Figure 6). The si419H treatment group (MSN-si419H weekly) produced relatively smaller tumors, with a 30% drop in bioluminescent signal after four weeks of therapy in comparison to the controls. The chemotherapy only treatment group (MSN-siQ and cisplatin weekly) had a reduction rate of about 50%, whereas the si419H with cisplatin chemotherapy treatment group (MSN-si419H and cisplatin weekly) exhibited an almost 85% decrease in tumor burden as measured by bioluminescence (Figure 6). Mice treated with MSN-siRNA twice weekly at half the dose failed to show these differences (data not shown).

Tumors collected from the MSN-si419H + cisplatin mice were significantly smaller when compared to the tumors from the MSN-siQ control mice (Figure 7, A and C). Furthermore, MSN-siQ control mice produced large numbers of disseminated masses and had enlarged primary tumors (Figure 7, A and B) in comparison to the MSN-si419H + cisplatin treated mice that exhibited no large disseminated lesions. It is important to note that cisplatin + MSN-siQ hindered tumor growth by more than 50% (Figure 7, B and C). However, si419H and cisplatin combination therapy inhibited Ovcar8-IP tumor growth to an even greater degree, with almost a 75% drop in number of foci and tumor weight in comparison to the controls (Figure 7, B and C). A similar trend was seen for proportion of mice developing

ascites, with 4/4 MSN-siQ and MSN-si419H treated mice, 2/4 cisplatin treated mice, and 1/4 combination treated mouse developing ascites. There was significant reduction in weight (p=0.0084) and number (p=0.0046) of disseminated masses between cisplatin + MSN-siQ and cisplatin + MSN-si419H treated mice, but this trend did not reach statistical significance for total tumor weight (p=0.1183). This is likely the result of greater MSN-siRNA uptake by the disseminated masses than primary tumor (Figure 6B).

Discussion

To our knowledge, this is the first example of silencing TWIST utilizing a nanoparticle delivery system in EOC. We demonstrate delivery and efficacy of chemically modified siRNA against TWIST in EOC; significant TWIST knockdown was achieved with a modified third generation PAMAM dendrimer and a silica nanoparticle *in vitro.* TWIST was chosen as a target for our siRNA approach because TWIST and its target genes have been shown to be highly affiliated with metastasis, EMT, drug resistance, and poor prognosis [7,36–39]. Successful knockdown of TWIST leads to a decrease in motility, followed by an increase in chemotherapy sensitivity in ovarian cancer [39]. This effect has also been previously shown in other cancers [15,40]. The delivery of our siRNA by YTZ3–15 was shown to have a profound effect on both TWIST silencing and chemoresistance in the EOC model. Silencing TWIST via the YTZ3–15 dendrimer substantially increased chemosensitivity, decreasing cell survival by more than 50% (Figure 2E). These data add to the growing evidence that TWIST is a clinically significant therapeutic target.

The PEI coated MSNs developed for this study successfully delivered siRNA into Ovcar8-IP ovarian cancer cells *in vitro* (Figure 4). This delivery also led to substantial knockdown of TWIST (Figure 4C). Our results demonstrate si419H's efficacy both *in vitro* and *in vivo.* Fluorescence microscopy demonstrated appropriate localization of MSN + Alexa-647 labeled siRNA in the lysosomes of EOC cells (Figure 4B), which lead to successful silencing of TWIST within 24 hours and complete absence of expression within one week (Figure 4C). As with YTZ3–15 delivery, MSN-delivered si419H sensitized EOC cells to cisplatin treatment (Figure 4D). *In vivo*, delivery of TWIST siRNA leads to significant impediment of metastatic growth in siTWIST treated mice in combination with cisplatin, reducing tumor weight almost 80% (Figure 7), compared to the siQ control. The observed decrease in tumor burden is mostly due to abrogated TWIST expression in EMT-mediated disseminated masses. These findings strongly support our assertion that TWIST is an important therapeutic target in EOC.

One of the main advantages of our system is its safety and specificity. The MSN-siRNA only localized to tumor sites and no other tissues or organs. It has previously been shown that the MSNs' size (120 nm) allows intravenously administered nanoparticles to escape through leaky vascular structure at the tumor site through the enhanced permeability and retention effect [41–43], however the mechanism for the observed tumor specificity following IP injection is under current investigation. It has been shown that PEI coating on the particle facilitates MSN uptake into tumor cells [44]. It is also possible that MSN uptake by tumor associated macrophages may be partially responsible for the tumor targeting and efficacy we have seen, however further research is needed to confirm this. The IP route of

administration is making gains in human trials and isnideal for TWIST targeting, as TWIST is silenced in adult tissues in the peritoneal cavity, limiting on-target, off-tumor effects of the siRNA strategy. Furthermore, our study corroborates earlier reports that MSNs are well tolerated and non-toxic at the concentrations used here [14,45,46]. Analysis of peritoneal organs at necropsy suggested no harmful effects to the specimens, as determined by a certified veterinary pathologist. However, additional experimentation is needed to evaluate the possible side effects of siRNA therapy including immune stimulation and off-target responses, which may be factors in this approach to cancer treatment [29,47].

The potential for these MSNs is vast due to their mesoporous nature as compared to other dense nanoparticles, such as gold or carbon. Additional studies will focus on exploiting the MSN pore structure, including the ability to create nanovalves on the surface of MSNs that provide an open/close function in order for anticancer drugs to be stored in the pores. Drugs are released when MSNs encounter conditions that open the valves, such as low pH or an external stimulus such as an oscillating magnetic field [23–28]. MSNs can also be modified with targeting moieties such as hyaluronic acid (HA). Since HA is a native ligand for CD44, which is overexpressed and correlates with worse prognosis in EOC [48,49], we hypothesize this will lead to enhanced uptake into tumors, especially in primary tumors, which in this study showed limited siRNA uptake *in vivo*.

Overall, this project serves to demonstrate that an MSN-siRNA approach can provide significant benefit in an EOC model, and sets the stage for future advances for IP delivery of therapeutics for EOC. Future work will focus on multifunctional MSNs, incorporating cytotoxic drug delivery and targeting moieties, in multiple cancer models.

Acknowledgements

The authors wish to thank our summer students, Evan, Bryonna and Leslie for their assistance with these experiments. We thank the Animal Tumor Model Core, particularly Indu Nair and Dr. Jun Wu, for assistance with *in vivo* studies. We also thank Brian Armstrong and the Light Microscopy and Digital Imaging Core at City of Hope for their assistance with confocal microscopy. Dr. Steven Vonderfecht performed pathological analysis on mouse specimens. Dr. Paul Burke advised on the chemical modification of siRNA. YTZ3–15 dendrimer was a gift from the Rossi Lab at City of Hope. A2780R cells were a gift from the laboratory of Susan Kane.

Funding:

This work was funded by a City of Hope Excellence Award (Glackin), Parvin Family Foundation (CAG), National Institutes of Health (NIH) (JIZ and FT). Research reported in this publication included work performed in CCSG Core facilities supported by the NCI/NIH under award number P30CA033572. The content is solely the responsibility of the authors and does not necessarily represent the official views of the NIH.

Abbreviations

EOC	Epithelial ovarian cancer
EMT	Epithelial to mesenchymal transition
PAMAM	Polyamidoamine
PEI	Polyethyleneimine
MSN	Mesoporous silica naoparticle

siQ	Control siRNA
CTAB	cetyltrimethylammonium bromide
siRNA	Small interfering RNA
SRB	Sulphorhodamine B
NSG	NOD.Cg-*Prkdc*^{scid}*Il2rg*^{tm1Wjl}/SzJ
IP	Intraperitoneal
GFP	Green Fluorescent Protein
Ffluc	Firefly Luciferase
RISC	RNA Induced Silencing Complex

References

1. Siegel RL, Miller KD & Jemal A Cancer statistics, 2016. CA: a cancer journal for clinicians 66, 7–30, doi:10.3322/caac.21332 (2016). [PubMed: 26742998]
2. Khalil I, Brewer MA, Neyarapally T & Runowicz CD The potential of biologic network models in understanding the etiopathogenesis of ovarian cancer. Gynecol Oncol 116, 282–285, doi:10.1016/j.ygyno.2009.10.085 (2010). [PubMed: 19931138]
3. Visintin I et al. Diagnostic markers for early detection of ovarian cancer. Clin Cancer Res 14, 1065–1072, doi:10.1158/1078-0432.ccr-07-1569 (2008). [PubMed: 18258665]
4. Karimi-Zarchi M et al. The Clinicopathologic Characteristics and 5-year Survival Rate of Epithelial Ovarian Cancer in Yazd, Iran. Electronic physician 7, 1399–1406, doi:10.14661/1399 (2015). [PubMed: 26516450]
5. Holschneider CH & Berek JS Ovarian cancer: epidemiology, biology, and prognostic factors. Seminars in surgical oncology 19, 3–10 (2000). [PubMed: 10883018]
6. Terauchi M et al. Possible involvement of TWIST in enhanced peritoneal metastasis of epithelial ovarian carcinoma. Clin Exp Metastasis 24, 329–339, doi:10.1007/s10585-007-9070-1 [doi] (2007). [PubMed: 17487558]
7. Yang J et al. Twist, a master regulator of morphogenesis, plays an essential role in tumor metastasis. Cell 117, 927–939, doi:10.1016/j.cell.2004.06.006 [doi] S0092867404005768 [pii] (2004). [PubMed: 15210113]
8. Yin G et al. Constitutive proteasomal degradation of TWIST-1 in epithelial-ovarian cancer stem cells impacts differentiation and metastatic potential. Oncogene 32, 39–49, doi:onc201233 [pii] 10.1038/onc.2012.33 [doi] (2013). [PubMed: 22349827]
9. Gort EH et al. Methylation of the TWIST1 promoter, TWIST1 mRNA levels, and immunohistochemical expression of TWIST1 in breast cancer. Cancer epidemiology, biomarkers & prevention : a publication of the American Association for Cancer Research, cosponsored by the American Society of Preventive Oncology 17, 3325–3330, doi:10.1158/1055-9965.epi-08-0472 (2008).
10. Vesuna F, Lisok A, Kimble B & Raman V Twist modulates breast cancer stem cells by transcriptional regulation of CD24 expression. Neoplasia (New York, N.Y.) 11, 1318–1328 (2009).
11. Yin G et al. TWISTing stemness, inflammation and proliferation of epithelial ovarian cancer cells through MIR199A2/214. Oncogene 29, 3545–3553, doi:10.1038/onc.2010.111 (2010). [PubMed: 20400975]
12. Ahmed N, Abubaker K, Findlay J & Quinn M Epithelial mesenchymal transition and cancer stem cell-like phenotypes facilitate chemoresistance in recurrent ovarian cancer. Current cancer drug targets 10, 268–278 (2010). [PubMed: 20370691]

13. Li S et al. TWIST1 associates with NF-kappaB subunit RELA via carboxyl-terminal WR domain to promote cell autonomous invasion through IL8 production. BMC Biol 10, 73, doi:1741–7007-10–73 [pii] 10.1186/1741-7007-10-73 [doi] (2012). [PubMed: 22891766]

14. Finlay J et al. Mesoporous silica nanoparticle delivery of chemically modified siRNA against TWIST1 leads to reduced tumor burden. Nanomedicine : nanotechnology, biology, and medicine 11, 1657–1666, doi:10.1016/j.nano.2015.05.011 (2015).

15. Finlay J et al. RNA-based TWIST1 inhibition via dendrimer complex to reduce breast cancer cell metastasis. BioMed research international 2015, 382745, doi:10.1155/2015/382745 (2015). [PubMed: 25759817]

16. Bobbin ML & Rossi JJ RNA Interference (RNAi)-Based Therapeutics: Delivering on the Promise? Annual review of pharmacology and toxicology 56, 103–122, doi:10.1146/annurev-pharmtox-010715-103633 (2016).

17. Brown CE et al. Recognition and killing of brain tumor stem-like initiating cells by CD8+ cytolytic T cells. Cancer Res 69, 8886–8893, doi:10.1158/0008-5472.can-09-2687 (2009). [PubMed: 19903840]

18. Yu T et al. An amphiphilic dendrimer for effective delivery of small interfering RNA and gene silencing in vitro and in vivo. Angew Chem Int Ed Engl 51, 8478–8484, doi:10.1002/anie.201203920 [doi] (2012). [PubMed: 22829421]

19. Liu X et al. Adaptive amphiphilic dendrimer-based nanoassemblies as robust and versatile siRNA delivery systems. Angew Chem Int Ed Engl 53, 11822–11827, doi:10.1002/anie.201406764 (2014). [PubMed: 25219970]

20. Hom C et al. Mesoporous silica nanoparticles facilitate delivery of siRNA to shutdown signaling pathways in mammalian cells. Small (Weinheim an der Bergstrasse, Germany) 6, 1185–1190, doi:10.1002/smll.200901966 (2010).

21. Meng H et al. Use of size and a copolymer design feature to improve the biodistribution and the enhanced permeability and retention effect of doxorubicin-loaded mesoporous silica nanoparticles in a murine xenograft tumor model. ACS nano 5, 4131–4144, doi:10.1021/nn200809t (2011). [PubMed: 21524062]

22. Liong M et al. Multifunctional inorganic nanoparticles for imaging, targeting, and drug delivery. ACS nano 2, 889–896, doi:10.1021/nn800072t (2008). [PubMed: 19206485]

23. Tarn D, Xue M & Zink JI pH-responsive dual cargo delivery from mesoporous silica nanoparticles with a metal-latched nanogate. Inorganic chemistry 52, 2044–2049, doi:10.1021/ic3024265 (2013). [PubMed: 23391170]

24. Ambrogio MW, Thomas CR, Zhao YL, Zink JI & Stoddart JF Mechanized silica nanoparticles: a new frontier in theranostic nanomedicine. Accounts of chemical research 44, 903–913, doi:10.1021/ar200018x (2011). [PubMed: 21675720]

25. Lu J, Li Z, Zink JI & Tamanoi F In vivo tumor suppression efficacy of mesoporous silica nanoparticles-based drug-delivery system: enhanced efficacy by folate modification. Nanomedicine : nanotechnology, biology, and medicine 8, 212–220, doi:10.1016/j.nano.2011.06.002 (2012).

26. Thomas CR et al. Noninvasive remote-controlled release of drug molecules in vitro using magnetic actuation of mechanized nanoparticles. Journal of the American Chemical Society 132, 10623–10625, doi:10.1021/ja1022267 (2010). [PubMed: 20681678]

27. Dong J, Xue M & Zink JI Functioning of nanovalves on polymer coated mesoporous silica Nanoparticles. Nanoscale 5, 10300–10306, doi:10.1039/c3nr03442a (2013). [PubMed: 24056925]

28. Deng ZJ et al. Layer-by-layer nanoparticles for systemic codelivery of an anticancer drug and siRNA for potential triple-negative breast cancer treatment. ACS nano 7, 9571–9584, doi:10.1021/nn4047925 (2013). [PubMed: 24144228]

29. Forsbach A et al. Identification of RNA sequence motifs stimulating sequence-specific TLR8-dependent immune responses. Journal of immunology (Baltimore, Md. : 1950) 180, 3729–3738 (2008).

30. Behlke MA Chemical modification of siRNAs for in vivo use. Oligonucleotides 18, 305–319, doi:10.1089/oli.2008.0164 (2008). [PubMed: 19025401]

31. Czauderna F et al. Structural variations and stabilising modifications of synthetic siRNAs in mammalian cells. Nucleic Acids Res 31, 2705–2716 (2003). [PubMed: 12771196]
32. Domcke S, Sinha R, Levine DA, Sander C & Schultz N Evaluating cell lines as tumour models by comparison of genomic profiles. Nat Commun 4, 2126, doi:10.1038/ncomms3126 (2013). [PubMed: 23839242]
33. Lee Y et al. A candidate precursor to serous carcinoma that originates in the distal fallopian tube. The Journal of pathology 211, 26–35, doi:10.1002/path.2091 (2007). [PubMed: 17117391]
34. Medeiros F et al. The tubal fimbria is a preferred site for early adenocarcinoma in women with familial ovarian cancer syndrome. The American journal of surgical pathology 30, 230–236 (2006). [PubMed: 16434898]
35. Morin PJ & Weeraratna AT Genetically-defined ovarian cancer mouse models. The Journal of pathology 238, 180–184, doi:10.1002/path.4663 (2016). [PubMed: 26496815]
36. Helleman J, Smid M, Jansen MP, van der Burg ME & Berns EM Pathway analysis of gene lists associated with platinum-based chemotherapy resistance in ovarian cancer: the big picture. Gynecol Oncol 117, 170–176, doi:10.1016/j.ygyno.2010.01.010 (2010). [PubMed: 20132968]
37. Yoshida J et al. Changes in the expression of E-cadherin repressors, Snail, Slug, SIP1, and Twist, in the development and progression of ovarian carcinoma: the important role of Snail in ovarian tumorigenesis and progression. Medical molecular morphology 42, 82–91, doi:10.1007/s00795-008-0436-5 (2009). [PubMed: 19536615]
38. Zhu DJ et al. Twist1 is a potential prognostic marker for colorectal cancer and associated with chemoresistance. American journal of cancer research 5, 2000–2011 (2015). [PubMed: 26269759]
39. Zhu X et al. miR-186 regulation of Twist1 and ovarian cancer sensitivity to cisplatin. Oncogene 35, 323–332, doi:10.1038/onc.2015.84 (2016). [PubMed: 25867064]
40. Cheng GZ et al. Twist transcriptionally up-regulates AKT2 in breast cancer cells leading to increased migration, invasion, and resistance to paclitaxel. Cancer Res 67, 1979–1987, doi:67/5/1979 [pii] 10.1158/0008-5472.CAN-06-1479 [doi] (2007). [PubMed: 17332325]
41. Greish K Enhanced permeability and retention (EPR) effect for anticancer nanomedicine drug targeting. Methods Mol Biol 624, 25–37, doi:10.1007/978-1-60761-609-2_3 (2010). [PubMed: 20217587]
42. Biswas S & Torchilin VP Dendrimers for siRNA Delivery. Pharmaceuticals (Basel, Switzerland) 6, 161–183, doi:10.3390/ph6020161 (2013).
43. Maeda H, Sawa T & Konno T Mechanism of tumor-targeted delivery of macromolecular drugs, including the EPR effect in solid tumor and clinical overview of the prototype polymeric drug SMANCS. Journal of controlled release : official journal of the Controlled Release Society 74, 47–61 (2001). [PubMed: 11489482]
44. Xia T et al. Polyethyleneimine coating enhances the cellular uptake of mesoporous silica nanoparticles and allows safe delivery of siRNA and DNA constructs. ACS nano 3, 3273–3286, doi:10.1021/nn900918w (2009). [PubMed: 19739605]
45. Ferris DP et al. Synthesis of biomolecule-modified mesoporous silica nanoparticles for targeted hydrophobic drug delivery to cancer cells. Small (Weinheim an der Bergstrasse, Germany) 7, 1816–1826, doi:10.1002/smll.201002300 (2011).
46. Lu J, Liong M, Zink JI & Tamanoi F Mesoporous silica nanoparticles as a delivery system for hydrophobic anticancer drugs. Small (Weinheim an der Bergstrasse, Germany) 3, 1341–1346, doi:10.1002/smll.200700005 (2007).
47. Gaglione M & Messere A Recent progress in chemically modified siRNAs. Mini reviews in medicinal chemistry 10, 578–595 (2010). [PubMed: 20500149]
48. Elzarkaa AA et al. Clinical relevance of CD44 surface expression in advanced stage serous epithelial ovarian cancer: a prospective study. Journal of cancer research and clinical oncology 142, 949–958, doi:10.1007/s00432-016-2116-5 (2016). [PubMed: 26762850]
49. Kayastha S et al. Expression of the hyaluronan receptor, CD44S, in epithelial ovarian cancer is an independent predictor of survival. Clin Cancer Res 5, 1073–1076 (1999). [PubMed: 10353740]

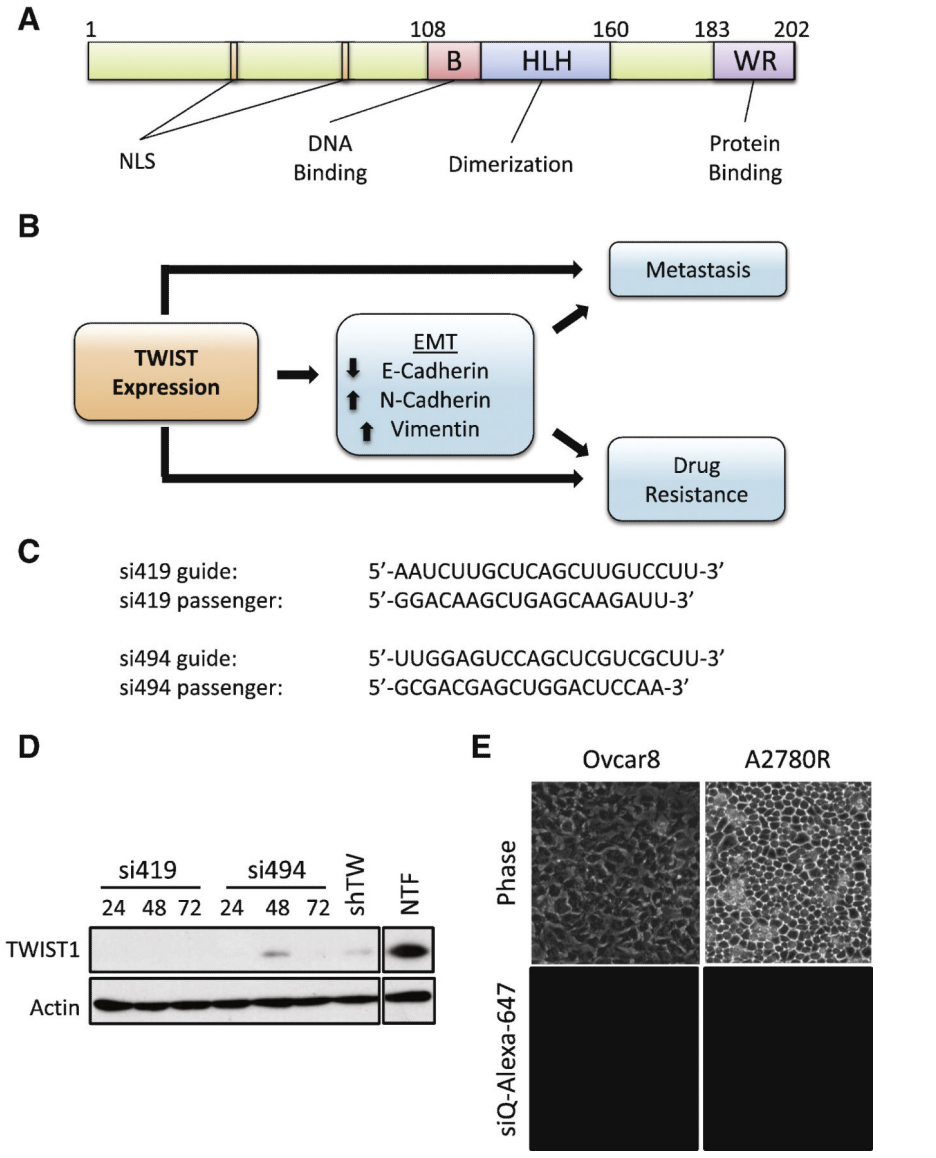

Figure 1.

A. TWIST schematic showing the basic DNA binding domain, helix-loop-helix dimerization motif, and C-terminal protein-binding WR domain. **B.** Reactivation of TWIST in cancers induces an epithelial to mesenchymal transition (EMT), which in turn has been shown to lead to metastasis and acquired drug resistance. **C.** Sequences of two TWIST siRNAs targeting the coding region of TWIST mRNA. **D.** Validation of siRNA. Lipofectamine 2000 was used to transfect A2780R cells with si419 or si494. Western blot reveals robust TWIST knockdown over three days post transfection. shRNA targeting TWIST is shown as a positive control for knockdown. **E.** Without a carrier, no siRNA enters target cells.

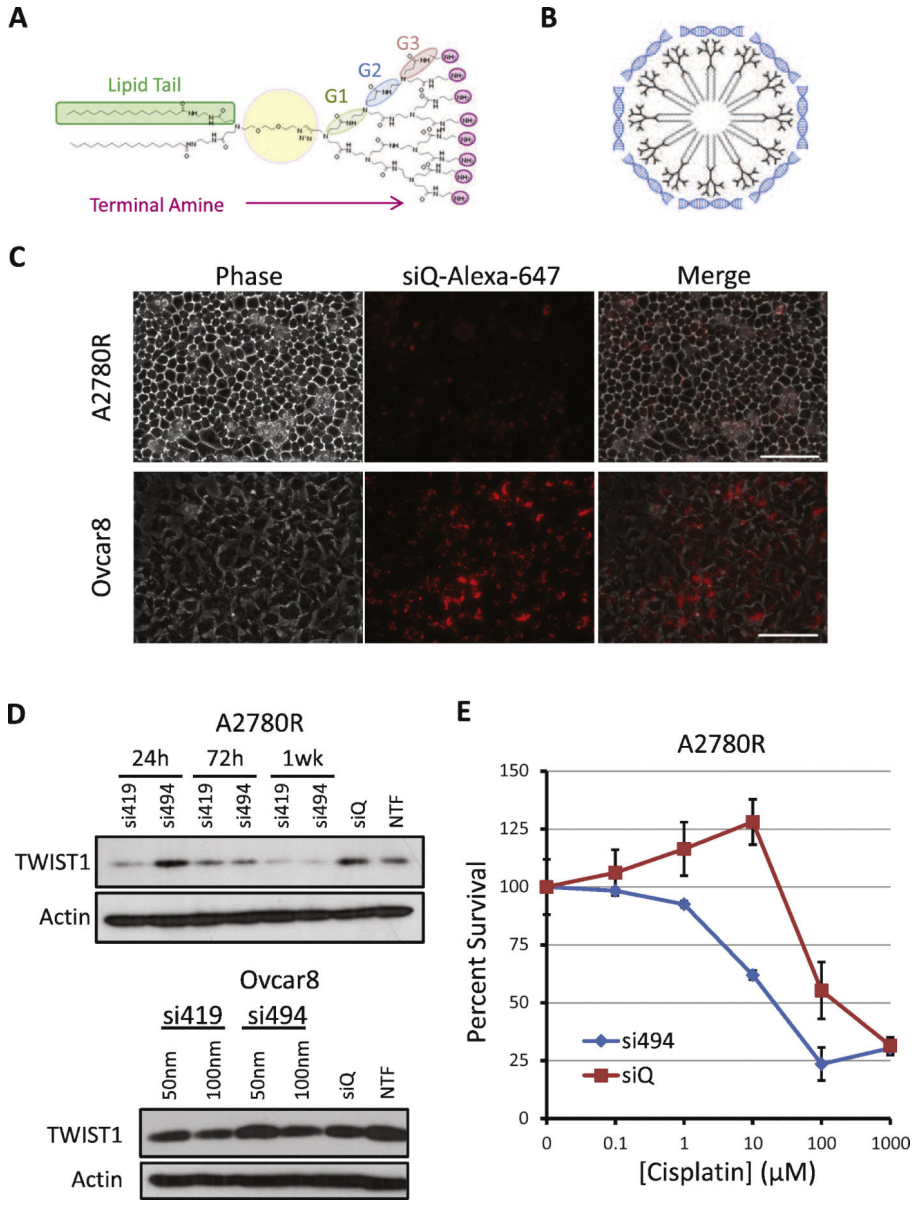

Figure 2.

A. YTZ3–15 PAMAM dendrimer used in these studies. Lipid tails (green) encourage formation of micelle structures once dendrimers are complexed with siRNA (**B.**), which is bound by terminal amines (pink). **C.** siQ control siRNA tagged with AlexaFluor-647 is efficiently taken up by A2780R and Ovcar8 cells. Scale bar, 100 μm. **D.** Both TWIST siRNAs, when delivered using YTZ3–15, result in knockdown of TWIST in A2780R cells, but even 100nM siRNA produces only minimal knockdown in Ovcar8. **E.** SRB assay reveals that A2780R cells are sensitized to cisplatin following treatment with YTZ3–15-si494 complexes. IC_{50} is reduced from ~200 to ~20 μM.

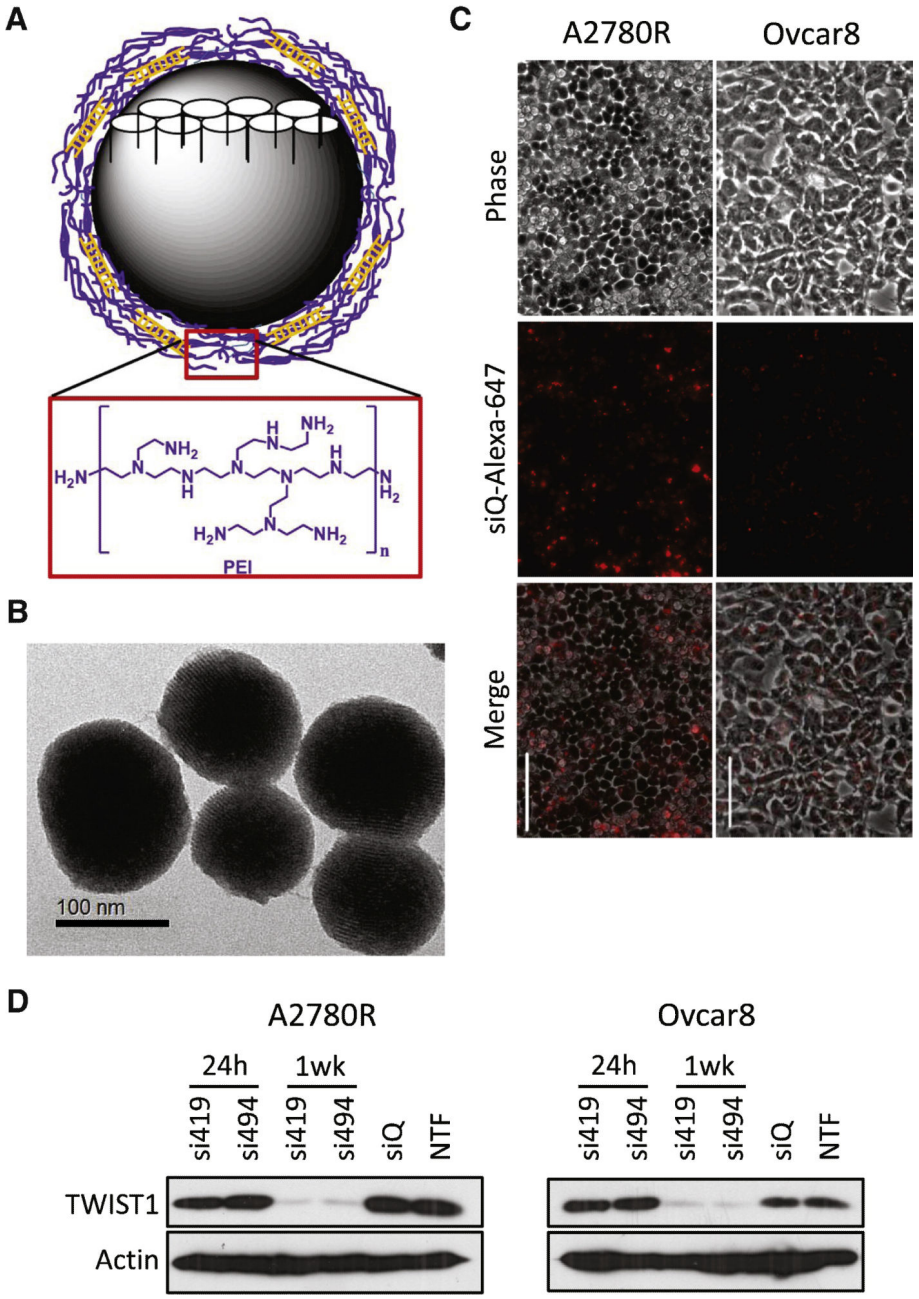

Figure 3.

A. Schematic of an MSN with pore structure (white). MSNs used in these studies have a PEI coating (purple layer) which binds siRNA (orange). Monomer structure for PEI is shown below. **B.** Transmission electron micrograph of MSNs. Particles are of uniform diameter, ~120 nm. **C.** A2780R and Ovcar8 cells efficiently take up MSNs loaded with siQ-AlexaFluor-647. Scale bar, 100 μm. **D.** In both cell lines, si419 and si494 loaded onto MSNs produce robust TWIST knockdown lasting one week post transfection, although TWIST protein remains at 24 hours post transfection.

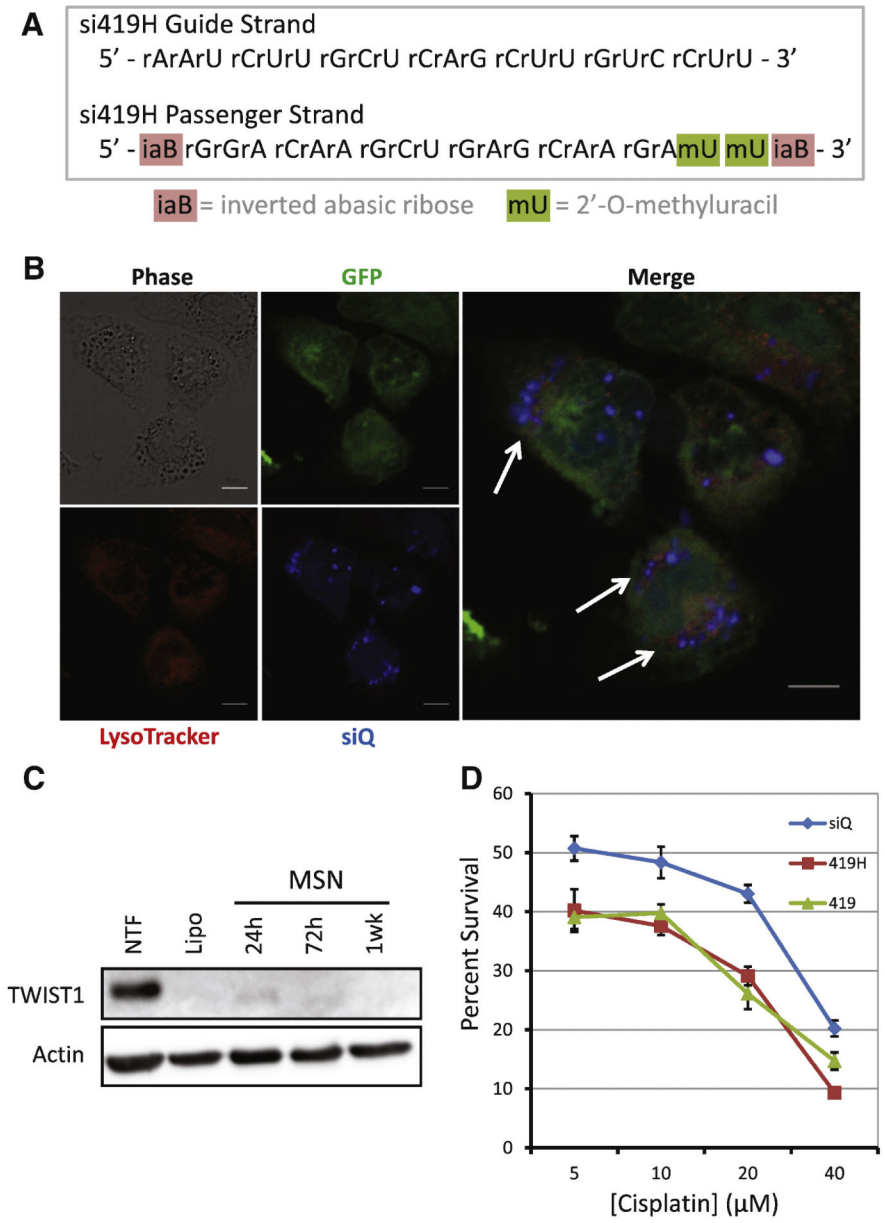

Figure 4.

A. In preparation for *in vivo* studies, si419 was chemically modified to include 2'-O-methyluracil and inverted abasic ribose caps on the passenger strand. This siRNA is termed si419H. **B.** Confocal microscopy demonstrates MSN delivery of siRNA to Ovcar8-IP cells. siQ-AlexaFluor-647 (blue) colocalizes with lysosomes and late endosomes, as stained by LysoTracker (red), reflecting proper trafficking of MSNs to allow siRNA release. **C.** Western blot confirms that si419H knocks down TWIST in Ovcar8-IP cells, including at the 24 hour timepoint. Knockdown is still effective one week post treatment. **D.** SRB cell survival assay reveals that TWIST knockdown sensitizes Ovcar8-IP cells to cisplatin. si419H performs similarly to unmodified si419. Ovcar8 is more sensitive than A2780R (Figure 2E), hence a less pronounced effect of TWIST on drug response in Ovcar8-IP.

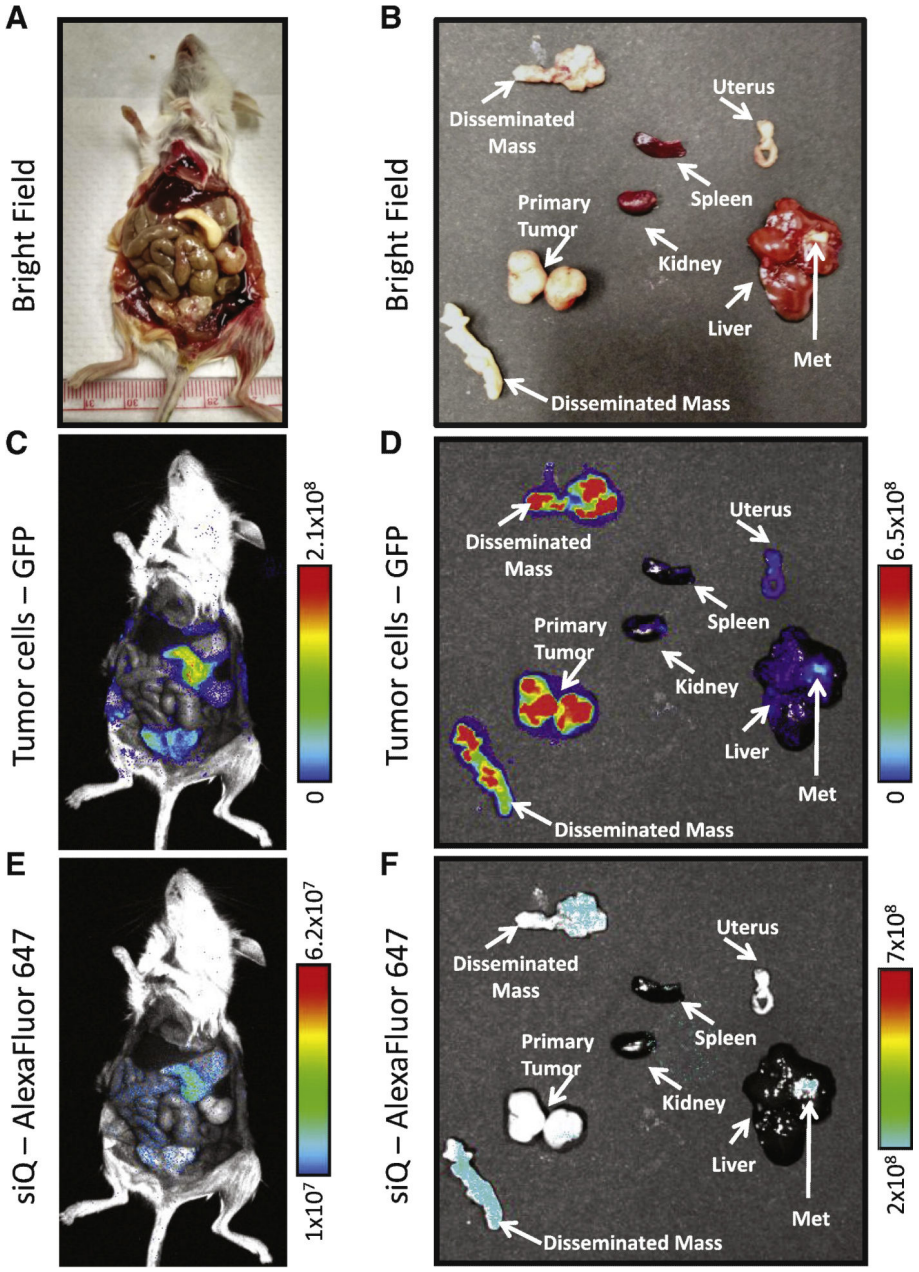

Figure 5.

A,C,E. Necropsy images of mice treated with siQ-AlexaFluor-647 on consecutive days reveal localization of MSN-siRNA complexes to the tumor. GFP fluorescence shows all Ovcar8-IP tumor cells within the abdominal cavity. siQ-AlexaFluor-647 fluorescence is concentrated in the large disseminated mass located near the stomach. **B,D,F.** Imaging of individual organs reveals that negligible quantities of MSNs are found in the uterus, liver, kidney, or spleen. siQ-AlexaFluor-647 fluorescence is mostly found in disseminated tumors, including a lesion on the liver surface, with limited signal from the primary tumor. Units for luminescence are photons/sec/cm^2/steradian.

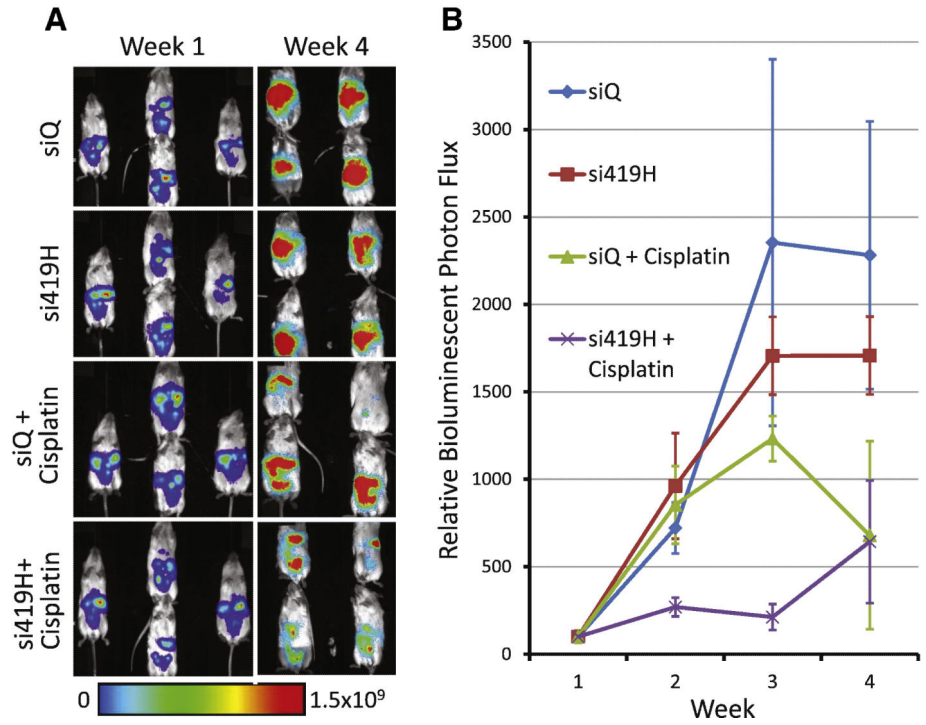

Figure 6.

A. Bioluminescence imaging of Ovcar8-IP tumors. Tumors treated with cisplatin plus MSN-siQ emit noticeably weaker signal than MSN-siQ only control mice, while those treated with cisplatin plus MSN-si419H exhibit a further loss of signal. **B.** Quantification of bioluminescence for all four weeks of treatment as depicted in A for weeks 1 and 4. Units for luminescence are photons/sec/cm^2/steradian.

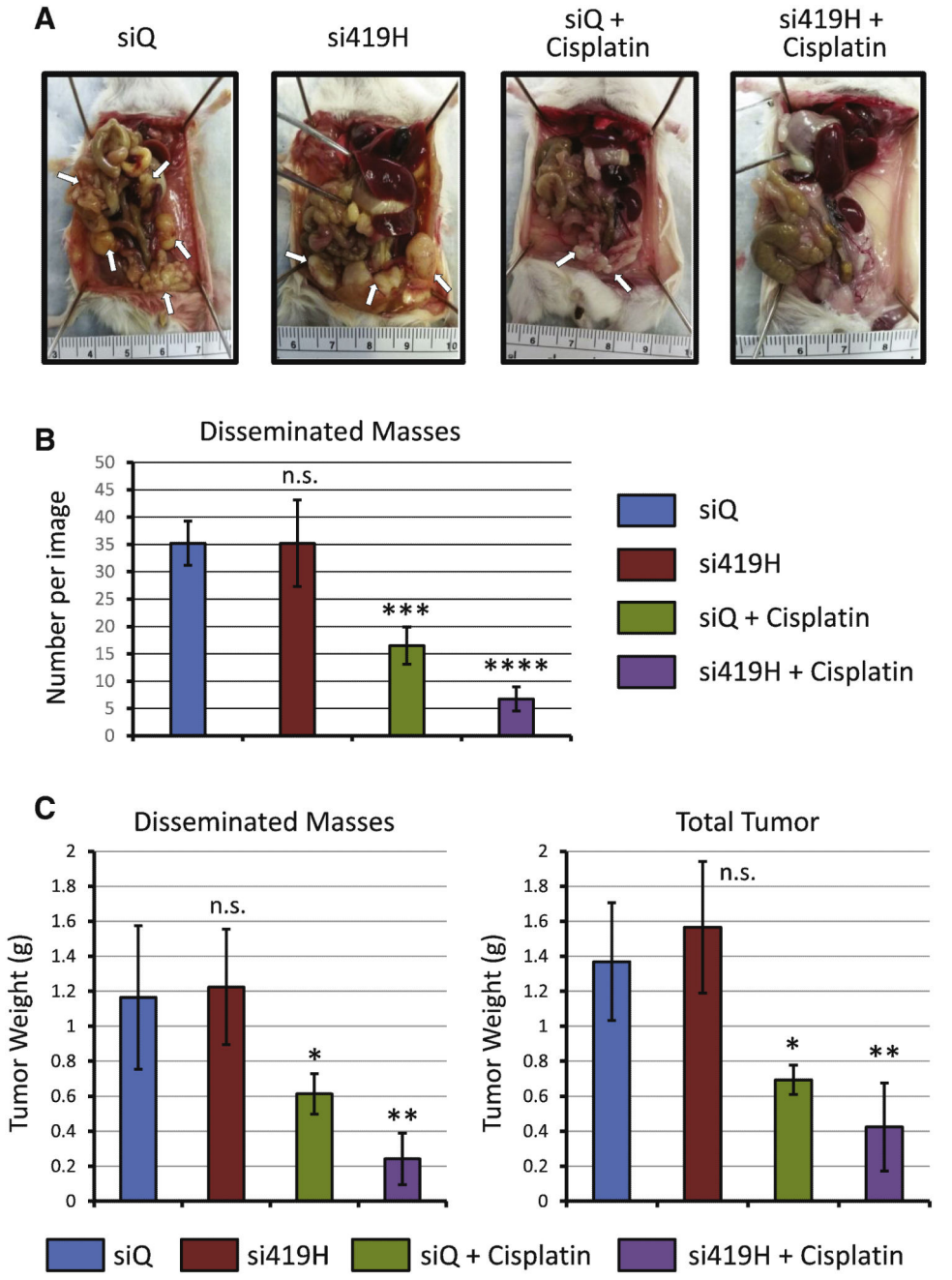

Figure 7.

A. Mice treated with MSN-siQ only have greater numbers and sizes of tumors than TWIST knockdown mice. Cisplatin treatment eliminated much of the tumor mass, but a combination of cisplatin and TWIST knockdown yielded the cleanest peritoneal cavity at the conclusion of the experiment. Arrows indicate tumor foci. One representative image shown per group (n=4). **B.** Quantification of numbers of disseminated masses seen in images of mice, as seen in A. Cisplatin treatment reduced metastasis incidence by approximately 50%, while combination of cisplatin with MSN-si419H reduced this 75%. **C.** Quantification of tumor weight for disseminated masses only (left) and total tumor including primary in ovaries

(right). Cisplatin, with or without TWIST knockdown, produced a significant drop in tumor weight. Addition of si419H led to a significant decrease in disseminated tumor mass ($p=0.0084$), and a drop in total tumor mass as well ($p=0.1183$). si419 alone did not produce a statistically significant change in tumor weight.